



# Benefits and trade-offs of optimizing global land use for food, water, and carbon

Anita D. Bayer<sup>a,1</sup> , Sven Lautenbach<sup>b,c,1,2</sup> , and Almut Arneth<sup>a,d</sup>

Edited by Hugh Possingham, The Nature Conservancy, Sherwood, QLD; received November 30, 2022; accepted August 5, 2023

Current large-scale patterns of land use reflect history, local traditions, and production costs, much more so than they reflect biophysical potential or global supply and demand for food and freshwater, or—more recently—climate change mitigation. We quantified alternative land-use allocations that consider trade-offs for these demands by combining a dynamic vegetation model and an optimization algorithm to determine Pareto-optimal land-use allocations under changing climate conditions in 2090–2099 and alternatively in 2033–2042. These form the outer bounds of the option space for global land-use transformation. Results show a potential to increase all three indicators (+83% in crop production, +8% in available runoff, and +3% in carbon storage globally) compared to the current land-use configuration, with clear land-use priority areas: Tropical and boreal forests were preserved, crops were produced in temperate regions, and pastures were preferentially allocated in semiarid grasslands and savannas. Transformations toward optimal land-use patterns would imply extensive reconfigurations and changes in land management, but the required annual land-use changes were nevertheless of similar magnitude as those suggested by established land-use change scenarios. The optimization results clearly show that large benefits could be achieved when land use is reconsidered under a “global supply” perspective with a regional focus that differs across the world’s regions in order to achieve the supply of key ecosystem services under the emerging global pressures.

land use | ecosystem services | biogeophysical limits | optimization | agricultural production

Given the growing human population and changes in per-capita consumption, large global pressures exist in the land system, reflecting the multiple—but diverse—benefits that human societies derive from the land (1). Historically, the increased demand for land-based commodities has been met by agricultural expansion into forests and other natural vegetation (2–4) combined with land-use intensification not least through technological developments (5). This resulted in high environmental costs, including greenhouse gas emission, biodiversity loss, and environmental pollution (1, 6, 7). With the continued increasing demand arising from a growing population and dietary shifts toward meat and dairy products, alongside moves toward climate change mitigation (e.g., biofuel production or large-scale forest area expansion), pressures continue to grow on our limited amount of land (1, 8, 9). The revenues of different land uses and their impacts, however, vary spatially given, for example, ecosystems’ differences in climate, soil fertility, and water availability (10–12). Therefore, an analysis of the revenues and impacts of the changes in land use required to address existing global pressures has to be spatially explicit.

Scenario analyses are routinely used to explore prospective socioeconomic and environmental changes in various futures of land use (13–16) and their impacts on ecosystems (17, 18). Scenarios are typically limited in number, and they rarely explore the bounds of the available option space. However, identifying absolute production limits of land-based commodities or services and suitable operating spaces of human interventions in the Earth’s ecosystems have been explored in recent years (19–22), among others with the planetary boundaries framework (23). In this context, also optimization approaches have been applied, which test out large numbers of configurations and, in doing so, can identify balances between trade-offs across multiple objectives, while simultaneously meeting additional constraints (such as bioclimatic limits or production demands) (21, 24). They aim at the identification of beneficial system states but without hard restrictions on how to reach the system state (e.g., the availability of adequate policy instruments or cultural and socioeconomic conditions). In the land-use sector, multiobjective optimization approaches have been used with a focus on ranking of sites for nature conservation (e.g., ref. 25) or with respect to land-use sharing versus land-use sparing (e.g., ref. 26). Optimizations targeting land use as such were applied on local to regional

## Significance

Food production often conflicts with carbon storage and freshwater supply. These trade-offs differ in space as they depend on biophysical constraints such as climate and soil properties. We explored the spatial pattern of trade-offs at the global scale and identified land-use configurations that would allow the simultaneous increase in global total carbon storage, food production, and freshwater supply. Reaching these configurations would require intensive land-use reconfigurations, but nevertheless, their extent is of similar magnitude as land-use changes assumed by widely used land-use scenarios. Therefore, the presented optimized land-use configurations help to identify global regions where the largest gains could be achieved for carbon storage, food production, and freshwater supply under changing climate and the need for climate change mitigation.

The authors declare no competing interest.

This article is a PNAS Direct Submission.

Copyright © 2023 the Author(s). Published by PNAS. This article is distributed under [Creative Commons Attribution-NonCommercial-NoDerivatives License 4.0 \(CC BY-NC-ND\)](https://creativecommons.org/licenses/by-nc-nd/4.0/).

Although PNAS asks authors to adhere to United Nations naming conventions for maps (<https://www.un.org/geospatial/mapsgeo/>), our policy is to publish maps as provided by the authors.

<sup>1</sup>A.D.B. and S.L. contributed equally to this work.

<sup>2</sup>To whom correspondence may be addressed. Email: [sven.lautenbach@heigit.org](mailto:sven.lautenbach@heigit.org).

This article contains supporting information online at <https://www.pnas.org/lookup/suppl/doi:10.1073/pnas.2220371120/-/DCSupplemental>.

Published October 9, 2023.

scale (e.g., refs. 27–33) and in a few studies also globally (e.g., refs. 34–38). These studies' results included predefined constraints (such as regional supply levels and persistence of current land-use classes) and did not consider climate change, with the exception of Pastor et al. (37).

Here, we optimized for the most prominent conflicting demands in the land-use sector to answer the question, how the global land-use configuration could look like by the end of the century when the biogeophysical potential is evaluated under the consideration of climate change. We targeted three key ecosystem service (ES) indicators: total carbon (C) storage (indicative of climate regulation and climate-change mitigation), crop production (indicative of food supply), and available runoff (indicative of freshwater supply) (“objectives,” see *SI Appendix, Fig. S1*). We used a state-of-the-art dynamic global vegetation model to simulate vegetation growth and crop yields, ecosystem C, and local water balances under historical and future climate (*Materials and Methods*). The ES indicators were then used in a multiobjective genetic optimization approach, which seeks to identify spatially explicit land-use allocations for which the global total of each of the three objectives could not increase further without declines in one of the other objectives. The optimizer was free to select one land use from potential natural vegetation, eight crop types, and pasture for each 1° gridcell of the global land surface. Only ES indicator provisioning of the current land-use configuration (as in 2017) was taken as the baseline constraint for the optimization to ensure that all solutions returned by the optimizer provide clear improvements. In contrast to previous studies, we did not apply additional constraints to the optimization in order to focus on exploring the biogeophysical maximum. Our optimization targeted environmental conditions under a low emission pathway (RCP 2.6, 39) at the end of the 21st century (2090–2099) to provide a long-term vision of land-use changes acknowledging the time scales needed for effective C storage and taking the impacts of climate change (CO<sub>2</sub> fertilization, changing temperatures, and precipitation) into account. To investigate the sensitivity of the results to different pathways and priorities, we repeated the analysis for a medium climate change pathway (RCP 6.0) and for a near to medium time perspective (15 y into the future). Our study aimed to 1) identify the outer bounds of ES indicator levels and land-use configurations that are biogeophysically realistic and adhere to the three competing major demands in the land-use sector and climate change, 2) identify priority areas for natural vs. agricultural land usage, and 3) to discuss the implications of achieving efficient land-use solutions, such as, for instance, land-use change needed, C emissions upon land-use change, and impacts on biodiversity.

### Global Land-Use Configurations Optimal for Three Key ES Indicators

The optimization resulted in a three-dimensional production-possibility frontier (also efficiency or Pareto frontier, Fig. 1) in which land-use allocations that were found to be “optimal” for the provision of total C storage, crop production, and available runoff are arranged based on their ES indicators' global totals. These solutions are henceforth referred to as optimal land-use configurations. The frontier reflects the inherent trade-offs between the three ES indicators and is spanned only by biogeophysical (i.e., vegetation growth) limitations and management options implemented in the LPJ-GUESS model. Reflecting the outer bounds of the option space, the frontier demonstrates the degree of inefficiency of all global land-use configurations with a total ES indicator provision lying below the frontier. This includes also

the land-use configuration as of 2017 (our reference for current land-use patterns; Fig. 1A, red diamond). Within the range of options spanned by the frontier, prioritization could be done by selecting subsets of solutions depending on further global or regional requirements, such as food supply levels or biodiversity targets.

The identified optimal land-use configurations show the theoretical potential for a significant simultaneous increase in all three objectives, aggregated globally, until the end of the century (2090–2099) under the low emission pathway RCP 2.6 relative to maintaining current land-use patterns. Global gains in ES indicators are given here as the average across solutions, but they reach their maximum with solutions prioritizing one over the other two ES indicators (i.e., solutions in the outer corners of the production-possibility frontier, see below). The optimized solutions indicated a ca. 3% increase, or ca. 38 Pg C, in C storage above the reference (average across solutions, see *SI Appendix, Table S4*, for details), or 98 Pg C (ca. 7% increase, when prioritized). Crop production increased by 83% in the cross-solution average relative to current land use but could be up to 210% when prioritized. The cross-solution average would be close to the necessary increase in agricultural production needed to feed the growing population by 2090–2099 (about 91% based on FAO values, *SI Appendix*). Gains in global available runoff were on average about 8% higher than the reference in 2090–2099 (13% when prioritized). For the medium climate change pathway (RCP 6.0), similar increases in all objectives were possible compared to the 2017 land use under the same climate (c.f. *SI Appendix, Table S4*): Averaged across the frontier, carbon storage increased by ca. 3%, crop production by ca. 80%, and available runoff by ca. 7%.

Likewise, when LPJ-GUESS was used with land-use projections used for IPCC assessments (LUH2, 40), ES indicator provision at the end of the century was also in most cases notably lower (*SI Appendix, Table S5 and Fig. S10*). This could be expected as in comparison to our theoretical, largely unconstrained land-use solutions, the scenarios used in IPCC are constrained by defined socioeconomic trajectories. Total C storage of a strong climate-change mitigation-based scenario, including significant amounts of reforestation and afforestation (SSP1-RCP2.6), was close to the average total C storage across the solutions from the optimization (1,381 Pg C in comparison to  $1,390 \pm 24$  Pg C across the optimal solutions and 1,352 Pg C when land use from 2017 would persist). However, crop production (22.4 vs.  $40.6 \pm 12.3$  and 22.2 Ecal) and available runoff (31,300 vs.  $36,200 \pm 900$  and 33,400 Pg H<sub>2</sub>O) were significantly lower compared to our production-possibility frontier. Results for a scenario assuming large population growth and cropland expansion (SSP3-RCP7.0) and another assuming high radiative forcing with little land-use change (SSP5-RCP8.5) were far below the frontier of efficient land-use configurations (compare *SI Appendix, Table S5*). While the Pareto-frontier results cannot be interpreted as being a “realistic” future of the world's land use, the comparison to trajectories that include socioeconomic constraints highlights the potentially achievable gains. Furthermore, it pinpoints where room toward enhanced ES provision is highest, if international policies could overcome some of today's obstacles underlying existing land-use patterns.

### Spatial Patterns of Optimal Land-Use Allocations

The optimization identified clear global priority areas for natural land, cropland, and pastures (Fig. 2A). Their broad pattern was very stable across the solutions on the production-possibility

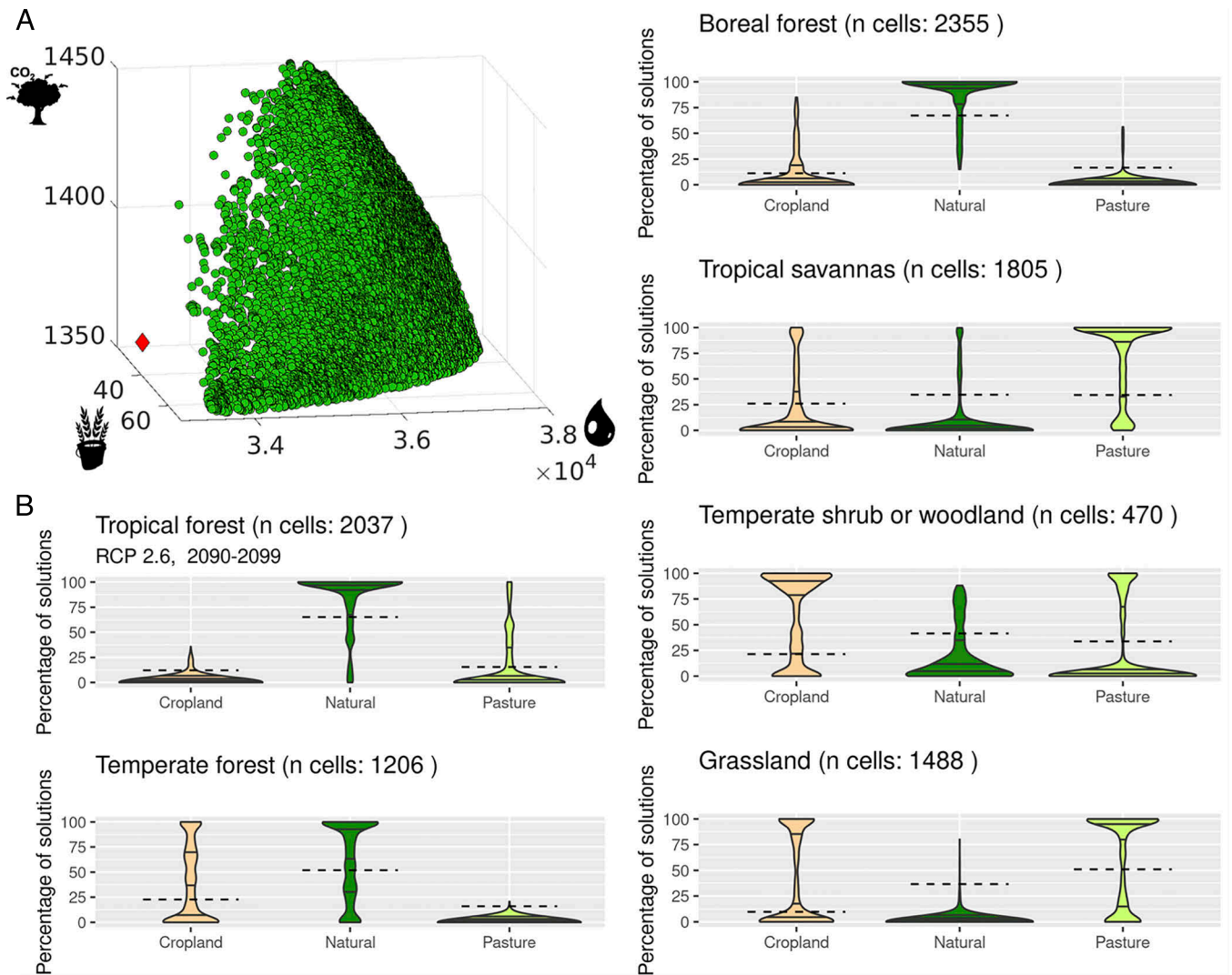


**Fig. 1.** Production-possibility frontier and optimal land use across biomes for the optimization targeting RCP 2.6 climate in 2090–2099. Solutions (green dots) locate on the efficiency frontier (A) based on their global total ES indicator provision of C storage (tree, Pg C), crop production (bucket, Ecal), and available runoff (drop, Pg H<sub>2</sub>O) with each solution representing one global land-use allocation. The point of origin (red diamond) is the ES indicator provision for the same climate and time period when land use is kept in the configuration of 2017 (reference of optimization runs, see *Materials and Methods*). See Fig. 3C for production-possibility frontiers of other combinations of RCPs and time horizons. The change in land uses allocated in the optimal solutions was classified per biome (B) and compared to the share of the land-use category under current land use (dashed lines). For each cell, the percentage of solutions for each scenario was calculated that had a specific land-use class allocated—a cell value of 50% for cropland implies that for 50% of the solutions across the production-possibility frontier, the cell was assigned cropland. Solid lines inside the violin plots indicate the 25th, 50th, and 75th percentiles of the distribution. No results are shown for tundra and desert biomes since only a very little number of cells were remaining in these biomes after the exclusion of cells where land-use change is prevented (*SI Appendix, section 2*). Biomes for 2008–2017 (*SI Appendix, Fig. S5*).

frontier with only small regional deviations for solutions focusing on selected parts of the frontier (Fig. 3B and *SI Appendix, Fig. S8*). Natural land use was assigned predominantly to tropical and boreal forest regions (Fig. 1B, see *SI Appendix, Fig. S5* for biome map) for the vast majority of solutions (Fig. 2C), reflecting the high C pools in tropical and boreal ecosystems (41). These results demonstrate the large climate change mitigation benefits achieved by maintaining and enhancing C storage in these regions (42). Some areas that would naturally be forested and are currently under agricultural land use were selected to return into forests, although not all regrowing forests would have reached the C storage under maturity by 2090–2099 (see *SI Appendix* and ref. 43). In temperate regions, where existing croplands would need to be significantly expanded to compensate for the regrowth of tropical and boreal natural ecosystems, e.g., the southern United States and Mexico, western Europe, South Africa, eastern China,

and also the coastal regions of Australia. Crop production in temperate regions was found to be the most efficient land use considering that 1) climate is favorable for crop growth and soils are of adequate quality, and 2) existing trade-offs with C storage and water provision are minimized. Selected cropland regions were only partly those with the highest computed yields globally since those regions were also of high importance for C storage. Concentrating croplands in areas with sufficient water available could help to greatly reduce the footprint of global agriculture, currently assessed to be responsible for more than 40% of freshwater usage (44). Trade-offs for fodder production in pastures were best exploited in subtropical to tropical grasslands and savannas, with about 79% being produced in these biomes.

There is broad congruence in spatial patterns between the identified optimal land-use configurations and the current land use, especially regarding the existence of natural land in the

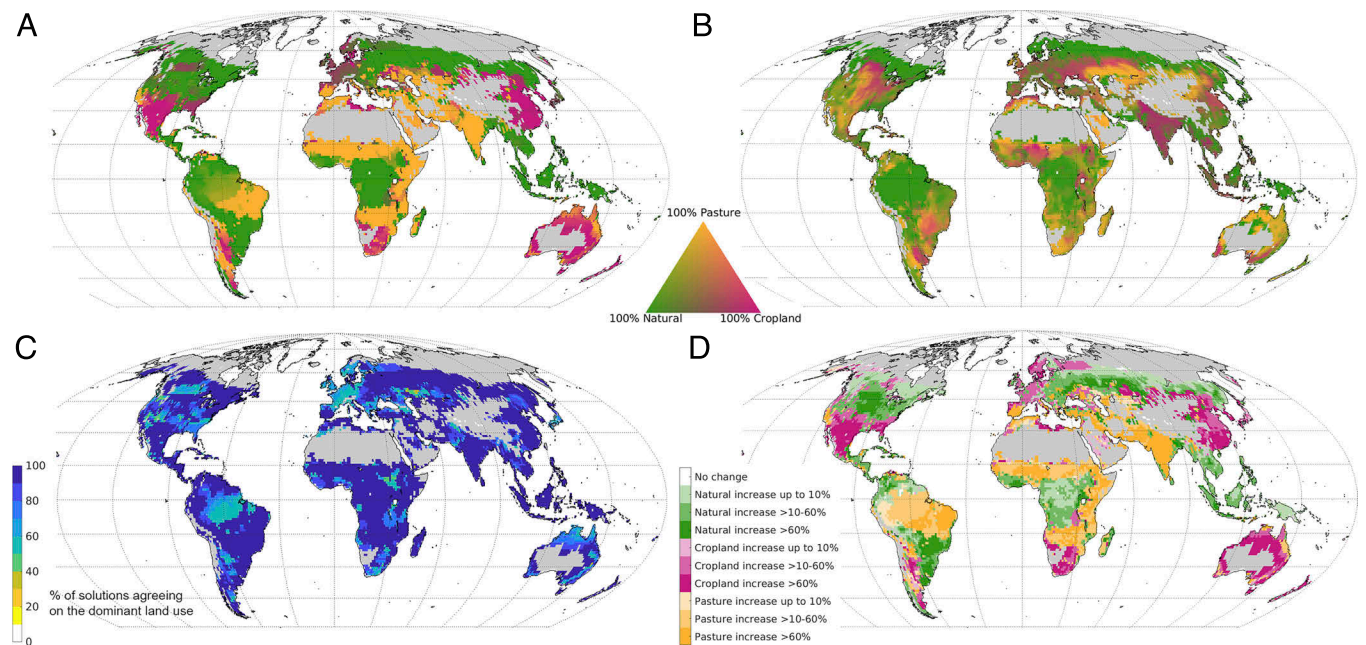


**Fig. 2.** Land-use priorities and the current land-use configuration. Global priority map for croplands, pasture, and natural regions derived from the optimization of land use for C storage, crop production, and available runoff targeting RCP2.6 climate in 2090–2099 (results are averaged across all solutions of the optimization, see *SI Appendix, Fig. S7* for other RCP and time horizon) (A). Current land-use configuration (as in 2017) in comparison (B). Panel (C) shows the percentage of solutions that agree on the dominant land use of each cell (as depicted in panel A) across all solutions of the optimization (e.g., 90–100% of solutions select the same land use in dark blue areas). Panel (D) shows the deviation of the optimized vs. the current land-use configuration. Note that in (A), the colors represent the distribution of the land uses selected for each gridcell across all solutions of the optimization (e.g., 80% of solutions picked natural and 20% cropland), with each solution just picking one land use per gridcell. In contrast, in (B), colors are real land-use fractions (e.g., 78% of the cell under natural land use and 22% cropland). Plots (A) and (B) share the triangle legend of land-use fractions. In (D), deviations in land-use patterns are categorized according to the legend below (although fractions in solutions are compared to real land-use fractions). Areas in gray were excluded from the optimization where land-use changes were limited by steep slopes or low productivity (*Materials and Methods* and *SI Appendix, section 3*).

forested biomes and pastures in semiarid regions (Fig. 2). The theoretically optimal land-use configurations (Fig. 2A, average across solutions) emerge as rather homogenous land-use patterns with clear boundaries between preferred land uses, which results from 1) the fact that solutions only indicate a single land use per gridcell instead of fractions, and 2) the >1,000 solutions strongly agreeing on the optimal land use for many grid cells (Fig. 2C and *SI Appendix, section 4*). By contrast, the current land-use pattern (Fig. 2B, real land-use fractions) with its mixed usage of the land in most grid locations reflects variable economic and social aspects of food production (e.g., local production vs. imports, adherence to traditions), which could not be reflected in our optimization without applying any further constraints beyond our consideration of biogeophysical conditions. Appreciable differences between current and optimized land use were found for India, subtropical Africa, and parts of the Amazon basin, regions for which the optimization suggested pasture, while the observed dominant land use in 2017 was cropland (India) and natural (Africa, South America). In the Amazon, the increases in pasture in the optimization reflect the drier conditions in this area by 2090–2099 projected by the four general circulation models (GCMs) used as climate input for the LPJ-GUESS simulations (*SI Appendix, Fig. S9*). The suggested massive cropland conversion to pasture in India, the Middle East, and Central Asia are in line with results by de Vrese et al. (12), who suggest a strong decline in agricultural productivity if irrigation practice would be reduced to sustainable levels in these regions. The optimization did not suggest an increase of croplands in higher latitudes where crop production is predicted to become feasible (12). For the eastern part of China, South Africa, Mexico, and the southern United States, cropland expansion

was suggested notably beyond what is currently found in these regions. Drastic land-use changes for such extended regions are unrealistic, but the results highlight where regional practices deviate most from globally theoretically achievable targets. For some regions, the identified land-use priorities correspond in spatial patterns and magnitude of changes with other, widely used projections of land use for the end of the century coming from land-use or integrated assessment models (see *SI Appendix, Fig. S11* for examples).

### Implications of Optimal Land-Use Configurations

Adjusting current global land use toward the theoretically optimal (given our three objectives) would imply substantial shifts in land use on about  $42.2\text{--}49.5 \cdot 10^6 \text{ km}^2$  (only between natural, cropland, and pasture, range across all solutions, see Fig. 1 and *SI Appendix, Table S4*). On average across solutions, nearly 2/3 of these transitions were suggested in developing countries vs. 1/3 in developed countries and countries in transition (country classification based on ref. 45). Total cropland area was  $10.7\text{--}25.4 \cdot 10^6 \text{ km}^2$  in comparison to currently about  $15.8 \cdot 10^6 \text{ km}^2$ . About 60% of the solutions lie within the identified planetary boundary of land used for crop production (23) ( $15\%$  or  $19.9 \cdot 10^6 \text{ km}^2$ ). The reconfiguration of land use could ultimately release about  $15.4\text{--}54.8 \text{ Pg C}$  (*SI Appendix, section 4*). For identified land-use configurations with the highest land-use change emissions, these would translate into  $0.67 \text{ Pg C/y}$  linearized annual rate and therefore be below current annual net emissions from land use and land-use change, which are estimated

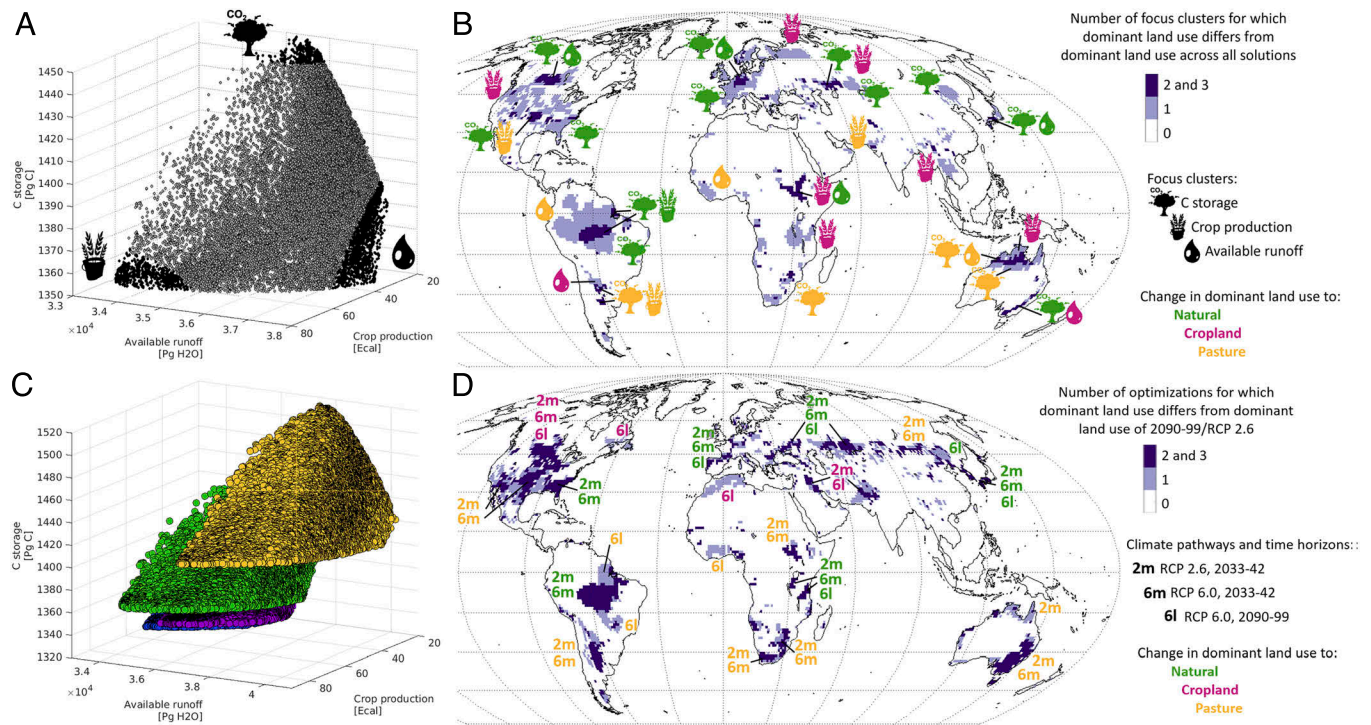


**Fig. 3.** Changes in land-use priorities across the range of the production-possibility frontier (A and B) and across climate pathways and time horizons (C and D). The upper panels compare the three clusters of solutions in the corners of the production-possibility frontier (A, i.e., providing higher C storage, crop production, and available runoff in comparison to the other two objectives) to the average result across all solutions for RCP 2.6 climate in 2090–2099. Solutions in the clusters were defined to provide >90% of the range of each ES indicator at the production efficiency frontier. The map (B) shows where the dominant land use across solutions in the focus clusters deviates from the dominant land use identified as average across all solutions. Icons refer to the three focus clusters and colors to the change in land use in this region. For instance, a green tree shows that the solutions providing higher C storage predominantly allocated natural land in this region in comparison to the average across all solutions which may be cropland or pasture. Compare *SI Appendix, Fig. S8* for land-use priorities of the three clusters. The lower panels (C and D) instead of solution clusters within one optimization compare the solutions from the optimization for RCP 2.6 climate in 2090–2099 (green frontier in C, see also *SI Appendix, Fig. S6*) to the three other combinations of climate pathways and time horizons. The map (D) compares the land-use priorities following the same scheme as in (B) (*SI Appendix, Fig. S7* for land-use priorities for all four combinations). For white areas, the dominant land use is identical across all four cases.

as  $1.6 \pm 0.7$  Pg C/y for 2010–2019 (46). Also, these emissions would partly be offset by some regrowth flux occurring in the years after the change, which is not included in our estimate. While we did not consider biodiversity as an objective of our optimization, we assessed biodiversity implications of the land-use configurations at the production-possibility frontier. To do so in a simplified way, we used a global-scale prioritization scheme for the protection of species and terrestrial ecoregions following Pouzols et al. (47) as an indicator. In their scheme, higher gridcell values indicate a higher value of the respective area for the protection of threatened species and ecoregions; therefore, higher global averages would indicate configurations that are assumed to be beneficial for biodiversity (see *SI Appendix* for details and caveats). Here, we found global averages of this indicator of 0.26–0.34 for the optimized land use in 2090–2099 with an average across solutions (0.29) similar to the indicator level for the current land-use configuration (0.30).

The implications of optimal land-use configurations were highly variant across the production-possibility frontier. For instance, in solutions providing higher levels of C storage in comparison to crop production and available runoff (see *SI Appendix* for analysis at the level of three focus clusters in the corners of the production-possibility frontier) where potential gains in C storage more than doubled compared to the average C gains across all solutions, natural land increased by 6.6% globally, and the global average biodiversity indicator increased by 14% in comparison to the average across solutions. In contrast, solutions

focusing on crop production nearly tripled crop production (compared to the +83% across all solutions) with associated reductions in the natural land fraction (–5.1%) and species protection (–0.03).

### Changes in Optimization Results for an Enhanced Climatic Pathway and a Shorter Time Horizon

Optimizations for a more pronounced climate change scenario (RCP 6.0) and for a near to medium time horizon (2033–2042) both changed levels of ES indicator provision (*SI Appendix, Table S4* for results of all four configurations) and resulted in small shifts in the land-use priorities (Fig. 3D and *SI Appendix, Fig. S7*). The solution space was smaller for the 2033–2042 optimization (for both RCPs), while it was wider when RCP 6.0 in 2090–2099 was targeted (see Fig. 3C for production-possibility frontiers of all four combinations). The latter results from the higher productivity of higher-latitude vegetation as a consequence of warmer temperatures, which opened up more possibilities for the optimization in these regions, as the eligibility of current land use declined even further requiring a stronger adjustment of future land use. However, all four combinations of time horizons and RCPs agree on the broad picture of the priority of land-use types (Fig. 2A, *SI Appendix, Fig. S7*, and white areas in Fig. 3D). These results suggest a robustness which would also emerge for a larger set of emission pathways.

## Conclusions and Challenges

In our analysis, we adopted a reduced-complexity approach, which is also a conservative one by assuming current day farming practices—if improvements in farming practice, such as an adaptation of crop varieties to climate change (*SI Appendix*), or technological improvements (48) would be considered, this might shift the production-possibility frontier to even higher levels. In contrast, an increase in the demand for other land resources (e.g., due to bioenergy growth or land-based climate-change mitigation) would reduce the option space for optimization (1). While the three objectives considered are of great importance for humanity, numerous other ES as well as socioeconomic factors determine real-world land-use decisions (49–52). Our purely biogeophysical perspective is designed to identify theoretical maxima under selected crucial trade-offs. Relocation of most of today's cropland clearly is not realistic, but our results add to the growing body of evidence that in regions where croplands are currently (and likely in future) less productive, potential exists for carbon uptake or biodiversity. Even much smaller changes in global land-use patterns toward those indicated here could thus attain globally significant cobenefits.

In general, we assumed the absence of trade barriers for both food and water—similar to assumptions made by Pastor et al. (37). Additional emissions by transport will lower the benefits with respect to increased carbon storage. However, food transport-related emissions tend to be relatively low (53, 54). Considering ES provision as a “global good,” especially in case of carbon uptake (with global climate benefits irrespective of the location it takes place) and crop production (which in principle can be transported between regions) requires a reliable international cooperation and governance of these goods. This would imply, e.g., a fair and functioning global trade network that supports adequate food supply for all under consideration of the water footprint of production, and the implementation of a carbon market, where climate regulation is traded with similar standards as food. Moreover, for livelihoods of local communities, the production of local food and the availability of water is essential in all world regions. Likewise, the existence of functioning protected area networks for nature conservation also is a local challenge (e.g., needs to exist also in temperate forests and savannas where the optimization suggests extended croplands). Still, local-scale strategies of resource use could need to be developed with global sustainability targets in mind. For instance, if food production would place a larger emphasis on a global land sparing strategy, larger regions in both tropical and boreal forest ecosystems could support for climate change mitigation with cobenefits to biodiversity. Given climate change impacts, enhanced crop production in temperate regions to satisfy global supply would be expected to be beneficial for water availability in drier regions through making water available for domestic use there that is now being used for irrigation.

Our results further strengthen previous work that highlighted the importance of conserving tropical and boreal forested regions for their unique climate regulation services (e.g., refs. 19, 41, and 55) and emphasize that crop and fodder production should be focused on temperate and subtropical regions (e.g., ref. 34). We show that this picture is robust under two climate change scenarios and in both scenarios is achieved by solely targeting biogeophysical potentials, without adding further constraints on land use (e.g., enforcing regional production levels). Using the three major demands in the land-use sector as a basis, our optimization provides the outer bounds of the space in which

land-use options operate. The production-possibility frontier leaves room for navigating on the frontier to meet any further global or regional requirements, such as food supply levels or biodiversity targets.

## Materials and Methods

We used the process-based global vegetation model LPJ-GUESS (56, 57) to simulate ecosystem dynamics and ES indicators for current and future land use. LPJ-GUESS has been shown to capture large-scale vegetation patterns, terrestrial carbon and nitrogen cycles, water balances, and crop yields (e.g., refs. 56, 58–60). LPJ-GUESS outputs were used as input to a genetic optimization algorithm seeking to find Pareto-optimal global land-use allocations (see *SI Appendix, Fig. S1* for workflow). Analyses were done on a 1° spatial grid, as a compromise between the necessary degree of detail and the processing time of the optimizer under these minimally constrained conditions in which the full option space of land-use allocations is explored.

**Modeling of Ecosystem Dynamics and Services.** Simulations ran from 1850 to 2099 and were driven by historical and future climate and atmospheric CO<sub>2</sub> concentration considering a low and a medium representative concentration pathway (RCPs 2.6 and 6.0, *SI Appendix, Fig. S9*) and bias-corrected projections from four GCMs (*SI Appendix, Table S2*). Historical simulations were needed as a basis for future projections of ecosystem functioning. The simulations (1850–2017) were based on reconstructed land use and climate, CO<sub>2</sub> and N-deposition as described in *SI Appendix, section 1*. For the future (2018–2099), reference simulations use future atmospheric climate and CO<sub>2</sub> forcing and keep land use as in 2017 to provide estimates for ES indicators under current land use but future climatic conditions. Ten additional simulations were run for the future period, assuming one individual land use to cover the entire globe: potential natural vegetation, four groups of the most common crop types (C3 cereals, C3 noncereal crops, C4 crops, and rice, see *SI Appendix, Table S1*; with each grown under both rainfed and irrigated conditions), and pasture. For each of the ten land-use options, we evaluated ES indicators C storage (total C pools in vegetation, litter, and soils), crop production (yields from LPJ-GUESS were scaled to FAO reported yields around the year 2000, see *SI Appendix*), and a proxy for available water, calculated as runoff minus twice the amount of water used for irrigation to take account of irrigation water losses (*SI Appendix*). This was done for a 10-y period at the end of the century (average of 2090–2099) and for a near to medium time horizon (~15 y from now, average of 2033–2042).

The crop growing area from the eight crop simulations was further limited according to the agro-ecological suitability data by FAO (<http://gazez.fao.org>, see *SI Appendix*) to include differences in microclimate, management, and soil fertility beyond the abilities of LPJ-GUESS. 1° cells with high fractions of slopes steeper than 30° or low production (*SI Appendix*) were excluded from the analysis because of their limited possibility for land-use change. Land use of areas under protection after UNEP and IUCN (categories Ia, Ib, and II after UNEP-WCMC, (61)) were fixed to natural vegetation so that they are not changeable in the optimization procedure. Details of these preprocessing steps and additional methods' information are given in *SI Appendix*.

**Optimization.** The optimization employed the nondominated sorting genetic algorithm NSGA-II (62) to estimate the set of Pareto-optimal solutions each consisting of a global land-use allocation of the 10 different land uses. The optimization did not consider fractions of land use but always allocated one land use to the 1° grid cells that formed the base for the calculation of the objectives. The objective function for the optimization consisted of the three ES indicators: sum of global crop production (Ecal), total C stored (Pg C), and available runoff (Pg H<sub>2</sub>O). C storage for climate regulation is effective on global scale and food products are traded globally, although with restrictions that depend, e.g., on durability and local supply. Water is transferred between regions by rivers and canals but typically not “traded” directly. We therefore do not account for regional supply levels but optimize for global totals on the assumption that higher levels of available water in general open up for other use opportunities

(domestic, industry, etc.). In addition, the following constraints were used: All objectives had to reach at least the value of the objective when land use in 2017 was continued, to limit the option space that is computationally explored to the space of interest. No additional constraints were set so to steer clear of ending up with interim solutions caused by enforcement of such constraints, but instead focusing on exploring the biogeophysical maximum. The productivity of pastures was accounted for by fodder production also being constrained to meet at least the production level when land use in 2017 was continued (see *SI Appendix* for further discussion). Given the huge search space, a hierarchical approach was used for the optimization. At the first stage, all combinations at the level of eight biomes (*SI Appendix*, Fig. S5) were evaluated and the set of Pareto-optimal solutions extracted (one land use per biome). These solutions were used as seed for the next stage at the level of food producing units (*SI Appendix*) intersected with biomes (764 spatial units). At this level of the optimization, NSGA-II was used with constraints lowered to 95% of the objectives in 2017. Results from the food producing units' level were used as seeds for the optimization at the level of 1° cells which used the objectives from 2017 as constraints. Constraint implementation across all levels followed Deb et al. (62): Solutions were first compared on the number of constraint violations and then on their objective function values. Solutions that violated constraints were thereby not excluded from the optimization but penalized. Especially in early stages of the optimization, this allows for a better performance and a higher diversity of solutions in the current population of solutions. Additional information is provided in *SI Appendix*.

**Data, Materials, and Software Availability.** Some study data available (Code for optimization and the input data for the optimization can be assessed at <https://github.com/slautenb/lpjguessOptim>) (63).

**ACKNOWLEDGMENTS.** This work was in parts funded by the European Commission's 7th Framework Program under Grant Agreement No. 308393 Operational Potential of Ecosystem Research Applications (OPERAs). This work was supported, in part, by the German Federal Ministry of Education and Research (BMBF) through the Helmholtz Association and its research program The Atmosphere in Global Change (ATMO). We thank the research groups for making their outputs available: Inter-Sectoral Impact Model Intercomparison Project (ISI-MIP) for climate model data, United Nations Environment Programme (UNEP) for protected area data, and Pouzols et al. for their research results. S.L. acknowledges support by the Klaus Tschira Stiftung.

Author affiliations: <sup>a</sup>Institute of Meteorology and Climate Research, Atmospheric Environmental Research (IMK-IFU), Global Land-Ecosystem Modelling group, Karlsruhe Institute of Technology, 82467 Garmisch-Partenkirchen, Germany; <sup>b</sup>Heidelberg Institute for Geoinformation Technology (HeiGIT) at Heidelberg University, 69118 Heidelberg, Germany; <sup>c</sup>GIScience Research Group, Heidelberg University, 69120 Heidelberg, Germany; and <sup>d</sup>Institute of Geography and Geoecology, Karlsruhe Institute of Technology, 76131 Karlsruhe, Germany

Author contributions: A.D.B., S.L., and A.A. designed research; A.D.B. and S.L. performed research; A.D.B. and S.L. contributed new reagents/analytic tools; A.D.B. and S.L. analyzed data; and A.D.B., S.L., and A.A. wrote the paper.

1. A. Arnet et al., "Framing and Context. Chapter 1" in *IPCC Special Report on Climate Change and Land*, P. R. Shukla, Eds. (Geneva, 2019), pp. 77–129.
2. E. C. Ellis et al., Used planet: A global history. *Proc. Natl. Acad. Sci. U.S.A.* **110**, 7978–7985 (2013).
3. R. L. Hooke, J. F. Martín Duque, J. D. Pedraza Gilsanz, Land transformation by humans: A review. *Ene* **12**, 43 (2013).
4. K. Klein Goldewijk, "A historical land use data set for the Holocene; HYDE 3.2" in *EGU General Assembly Conference Abstracts* (2016), p. EPSC2016-1574.
5. T. K. Rudel et al., Agricultural intensification and changes in cultivated areas, 1970–2005. *Proc. Natl. Acad. Sci. U.S.A.* **106**, 20675–20680 (2009).
6. S. Diaz et al., "Summary for policymakers of the global assessment report on biodiversity and ecosystem services of the intergovernmental science-policy platform on biodiversity and ecosystem services" (Tech. Rep., Intergovernmental Science-Policy Platform on Biodiversity and Ecosystem Services, 2019).
7. D. Tilman, K. G. Cassman, P. A. Matson, R. Naylor, S. Polasky, Agricultural sustainability and intensive production practices. *Nature* **418**, 671–677 (2002).
8. P. Alexander et al., Drivers for global agricultural land use change: The nexus of diet, population, yield and bioenergy. *Global Environ. Change* **35**, 138–147 (2015).
9. P. Alexander, C. Brown, A. Arneith, J. Finnigan, M. D. Rounsevell, Human appropriation of land for food: The role of diet. *Global Environ. Change* **41**, 88–98 (2016).
10. N. Ramankutty, J. A. Foley, J. Norman, K. McSweeney, The global distribution of cultivable lands: Current patterns and sensitivity to possible climate change. *Global Ecol. Biogeogr.* **11**, 377–392 (2002).
11. C. Dalin, I. Rodríguez-Iturbe, Environmental impacts of food trade via resource use and greenhouse gas emissions. *Environ. Res. Lett.* **11**, 035012 (2016).
12. P. de Vrese, T. Stacke, S. Hagemann, Exploring the biogeophysical limits of global food production under different climate change scenarios. *Earth Syst. Dyn.* **9**, 393–412 (2018).
13. P. Alexander et al., Assessing uncertainties in land cover projections. *Global Change Biol.* **23**, 767–781 (2017).
14. H. Mitter et al., Shared socio-economic pathways for European agriculture and food systems: The Eur-Agri-SSPs. *Global Environ. Change* **65**, 102159 (2020).
15. A. Popp et al., Land-use futures in the shared socio-economic pathways. *Global Environ. Change* **42**, 331–345 (2017).
16. C. Schmitz et al., Land-use change trajectories up to 2050: Insights from a global agro-economic model comparison. *Agric. Econ.* **45**, 69–84 (2014).
17. A. D. Bayer et al., Diverging land-use projections cause large variability in their impacts on ecosystems and related indicators for ecosystem services. *Earth Syst. Dyn.* **12**, 327–351 (2021).
18. S. S. Rabin et al., Impacts of future agricultural change on ecosystem service indicators. *Earth Syst. Dyn.* **11**, 357–376 (2020).
19. S. Franck, W. von Bloh, C. Müller, A. Bondeau, B. Sakschewski, Harvesting the sun: New estimations of the maximum population of planet earth. *Ecol. Modell.* **222**, 2019–2026 (2011).
20. J. F. Bastin et al., The global tree restoration potential. *Science* **365**, 76–79 (2019).
21. F. P. Smith, R. Gorddard, A. P. House, S. McIntyre, S. M. Prober, Biodiversity and agriculture: Production frontiers as a framework for exploring trade-offs and evaluating policy. *Environ. Sci. Policy* **23**, 85–94 (2012).
22. K. H. Erb et al., Exploring the biophysical option space for feeding the world without deforestation. *Nat. Commun.* **7**, 1–9 (2016).
23. J. Rockström et al., A safe operating space for humanity. *Nature* **461**, 472–475 (2009).
24. R. Seppelt, S. Lautenbach, M. Volk, Identifying trade-offs between ecosystem services, land use, and biodiversity: A plea for combining scenario analysis and optimization on different spatial scales. *Curr. Opin. Environ. Sust.* **5**, 458–463 (2013).
25. M. Jung et al., Areas of global importance for conserving terrestrial biodiversity, carbon and water. *Nat. Ecol. Evol.* **5**, 1499–1509 (2021).
26. R. K. Runting et al., Larger gains from improved management over sparing-sharing for tropical forests. *Nat. Sustain.* **2**, 53–61 (2019).
27. B. A. Bryan et al., Land use efficiency: Anticipating future demand for land-sector greenhouse gas emissions abatement and managing trade-offs with agriculture, water, and biodiversity. *Global Change Biol.* **21**, 4098–4114 (2015).
28. S. Lautenbach, M. Volk, M. Strauch, G. Whittaker, R. Seppelt, Optimization-based trade-off analysis of biodiesel crop production for managing an agricultural catchment. *Environ. Modell. Software* **48**, 98–112 (2013).
29. S. Polasky et al., Where to put things? Spatial land management to sustain biodiversity and economic returns. *Biol. Conserv.* **141**, 1505–1524 (2008).
30. W. Verhagen, E. H. van der Zanden, M. Strauch, A. J. van Teeffelen, P. H. Verburg, Optimizing the allocation of agri-environment measures to navigate the trade-offs between ecosystem services, biodiversity and agricultural production. *Environ. Sci. Policy* **84**, 186–196 (2018).
31. J. A. Versteegen et al., How a pareto frontier complements scenario projections in land use change impact assessment. *Environ. Modell. Software* **97**, 287–302 (2017).
32. E. A. Law et al., Fading opportunities for mitigating agriculture-environment trade-offs in a south American deforestation hotspot. *Biol. Conserv.* **262**, 109310 (2021).
33. C. M. Lemos, H. L. Beyer, R. K. Runting, P. R. Andrade, A. P. Aguiar, Multicriteria optimization to develop cost-effective pes-schemes to restore multiple environmental benefits in the Brazilian Atlantic forest. *Ecosyst. Serv.* **60**, 101515 (2023).
34. V. Heck, H. Hoff, S. Wirseniuss, C. Meyer, H. Kreft, Land use options for staying within the planetary boundaries-synergies and trade-offs between global and local sustainability goals. *Global Environ. Change* **49**, 73–84 (2018).
35. L. P. Koh, T. Koellner, J. Ghazoul, Transformative optimisation of agricultural land use to meet future food demands. *PeerJ* **1**, e188 (2013).
36. B. B. Strassburg et al., Global priority areas for ecosystem restoration. *Nature* **586**, 724–729 (2020).
37. A. V. Pastor et al., The global nexus of food-trade-water sustaining environmental flows by 2050. *Nat. Sust.* **2**, 499–507 (2019).
38. A. C. Castonguay et al., Navigating sustainability trade-offs in global beef production. *Nat. Sust.* **6**, 28–294 (2023).
39. D. P. Van Vuuren et al., The representative concentration pathways: An overview. *Climat. Change* **109**, 5–31 (2011).
40. G. C. Hurtt et al., Harmonization of global land use change and management for the period 850–2100 (LUH2) for CMIP6. *Geosci. Mod. Dev.* **13**, 5425–5464 (2020).
41. T. Tagesson et al., Recent divergence in the contributions of tropical and boreal forests to the terrestrial carbon sink. *Nat. Ecol. Evol.* **4**, 202–209 (2020).
42. K. J. Anderson-Teixeira et al., Climate-regulation services of natural and agricultural ecoregions of the Americas. *Nat. Clim. Change* **2**, 177–181 (2012).
43. A. Krause, T. A. Pugh, A. D. Bayer, M. Lindeskog, A. Arneith, Impacts of land-use history on the recovery of ecosystems after agricultural abandonment. *Earth Syst. Dyn.* **7**, 745–766 (2016).
44. OECD, "Trends and drivers of agri-environmental performance in OECD countries" (Tech. Rep., 2019).
45. United Nations, "The world economic situation and prospects (WESP): Country classification" (Tech. Rep., 2014).
46. P. Friedlingstein et al., Global carbon budget 2020. *Earth Syst. Sci. Data* **12**, 3269–3340 (2020).
47. F. M. Pouzols et al., Global protected area expansion is compromised by projected land-use and parochialism. *Nature* **516**, 383–386 (2014).

48. T. Wheeler, J. Von Braun, Climate change impacts on global food security. *Science* **341**, 508-513 (2013).
49. M. D. Rounsevell *et al.*, A biodiversity target based on species extinctions. *Science* **368**, 1193-1195 (2020).
50. U. Heink, J. Hauck, K. Jax, U. Sukopp, Requirements for the selection of ecosystem service indicators—The case of MAES indicators. *Ecol. Indic.* **61**, 18-26 (2016).
51. A. P. van Oudenhoven *et al.*, Key criteria for developing ecosystem service indicators to inform decision making. *Ecol. Indic.* **95**, 417-426 (2018).
52. T. Benton *et al.*, Designing sustainable land use in a 1.5°C world: The complexities of projecting multiple ecosystem services from land. *Curr. Opin. Environ. Sust.* **31**, 88-95 (2018).
53. A. Cristea, D. Hummels, L. Puzello, M. Avetisyan, Trade and the greenhouse gas emissions from international freight transport. *J. Environ. Econ. Manage.* **65**, 153-173 (2013).
54. U. Kreidenweis, S. Lautenbach, T. Koellner, Regional or global? The question of low-emission food sourcing addressed with spatial optimization modelling. *Environ. Modell. Software* **82**, 128-141 (2016).
55. J. G. Canadell, M. R. Raupach, Managing forests for climate change mitigation. *Science* **320**, 1456-1457 (2008).
56. S. Olin *et al.*, Modelling the response of yields and tissue C:N to changes in atmospheric CO<sub>2</sub> and N management in the main wheat regions of western Europe. *Biogeosciences* **12**, 2489-2515 (2015).
57. B. Smith *et al.*, Implications of incorporating N cycling and N limitations on primary production in an individual-based dynamic vegetation model. *Biogeosciences* **11**, 2027-2054 (2014).
58. D. Gerten, S. Schaphoff, U. Haberlandt, W. Lucht, S. Sitch, Terrestrial vegetation and water balance—Hydrological evaluation of a dynamic global vegetation model. *J. Hydrol.* **286**, 249-270 (2004).
59. T. Hickler *et al.*, Projecting the future distribution of European potential natural vegetation zones with a generalized, tree species-based dynamic vegetation model. *Global Ecol. Biogeogr.* **21**, 50-63 (2012).
60. S. Piao *et al.*, Evaluation of terrestrial carbon cycle models for their response to climate variability and to CO<sub>2</sub> trends. *Global Change Biol.* **19**, 2117-2132 (2013).
61. IUCN and UNEP-WCMC, *The World Database on Protected Areas - WDPA* (UNEP-WCMC, Cambridge, UK, 2015).
62. K. Deb, A. Pratap, S. Agarwal, T. Meyarivan, A fast and elitist multiobjective genetic algorithm: NSGA-II. *IEEE Trans. Evol. Comput.* **6**, 182-197 (2002).
63. S. Lautenbach, Source code and data for Bayer, Lautenbach, Arneth Benefits and trade-offs of optimizing global land use for food, water, and carbon. GitHub. <https://github.com/slautenb/lpjguessOptim/tree/main/data>. Accessed 15 September 2023.